Macromolecules

pubs.acs.org/Macromolecules Article

Associating Polymers in the Strong Interaction Regime: Validation of the Bond Lifetime Renormalization Model

Sirui Ge, Gregory Peyton Carden, Subarna Samanta, Bingrui Li, Ivan Popov, Peng-Fei Cao, and Alexei P. Sokolov*

Cite This: *Macromolecules* 2023, 56, 2397−2405 Read Online

ACCESS | Metrics & More | Article Recommendations | Supporting Information

ABSTRACT: Quantitative understanding of dynamics and viscoelastic properties of associating polymers remains a challenge. This study presents detailed analysis of dielectric and rheological data for telechelic PDMS functionalized with two different end groups, urea that forms multiple hydrogen bonds and carboxylic acid that forms much weaker hydrogen bonds. Analysis of the results revealed that the bond dissociation and bond rearrangement times are similar in the case of strong bonding urea-functionalized samples but are different in the case of weaker interacting carboxylic acid end groups. We demonstrate that these results agree well with the predictions of the bond lifetime renormalization model. The presented results suggest that rheological data can be used for the estimation of activation energy for bond dissociation only in the strong interaction regime and that segmental relaxation should be explicitly accounted for in these estimates, at least, in the systems studied herein.

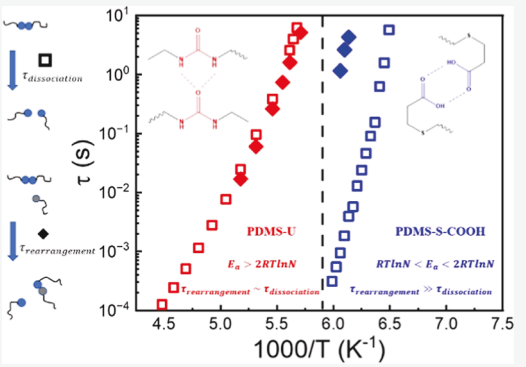

INTRODUCTION

Associating polymers present an interesting class of materials with many unique properties.[1−3] This field was inspired by a large variety of non-covalent interactions prevalent in natural materials, and synthetic chemists used these transient bonds (hydrogen bonds,[4] ionic bonds,[5] metal−ligand coordination,[6] $\pi-\pi$ stacking,[7] etc.) to convert conventional polymers to be more dynamic in nature, enabling intrinsic self-healing ability[8,9] and easy processability,[10] along with strong improvements in toughness,[11,12] adhesion,[13,14] and many other properties.[15] The range of transient bond dissociation energy E_a varies depending on the type of interaction, and this energy controls the characteristic time scale and temperature range of their association−dissociation process.[16] The most common interaction type found in nature is based on H-bonding. Although a single H-bond has a low energy barrier for dissociation, E_a ∼6−8 kJ/mol,[17−19] the combined strength of multiple H-bonding can provide superior mechanical robustness to a low-molecular-weight polymer without the aid of permanent cross-linking.

The lifetime of dynamic bonds is one of the key factors controlling the viscoelastic properties and self-healing kinetics.[16,20,21] The transient network persists at a time scale shorter than the lifetime of the transient bonds, whereas at longer times, dynamic bonds dissociate and polymer chains become free to move, leading to network rearrangement. Previous experiments in well-defined telechelic polymeric systems with H-bonded functional groups indicate that the time scale of the network rearrangement and the bond-dissociation time scale measured by dielectric spectroscopy are not the same.[19,22,23] Essentially, there are two characteristic times: bond dissociation time and bond rearrangement time, and they might be significantly different.[19] This discrepancy has been explained by the Bond Lifetime Renormalization Model introduced by Stukalin et al.[24] to describe the mechanism of self-healing kinetics. According to this model, the above-mentioned time scale difference arises because a dissociated sticker can reassociate with its original partner several times before binding to a new partner. Stress relaxation occurs only when the sticker changes the partner (bond rearrangement event). However, this behavior is predicted only for the intermediate bond-energy regime, $RT\ \ln(N) < E_a < 2RT\ \ln(N)$, where N denotes the number of polymer segments. In this regime, the bond lifetime is short and, as a result, there are plenty of open stickers in the volume pervaded by the dangling chain. Open stickers follow a compact space exploration via sub-diffusive Rouse motion resulting in the bond formation with the same partner again and again. This mechanism has been verified and confirmed experimentally.[19,22,25]

On the other hand, the model predicts a different behavior at higher dissociation energy, when $E_a > 2RT\ \ln N$. With higher bond strength, most of the stickers are in the bonded state for a

Received: December 2, 2022
Revised: January 31, 2023
Published: March 10, 2023

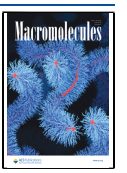

https://doi.org/10.1021/acs.macromol.2c02446
Macromolecules 2023, 56, 2397−2405

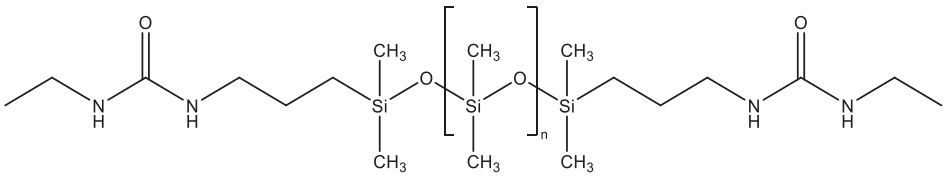

PDMS-U (DP = 22 and 50)

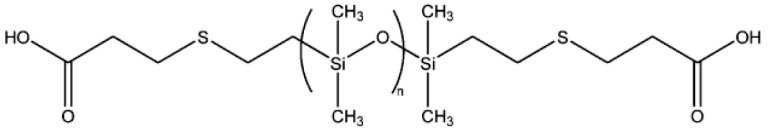

PDMS-S-COOH (DP = 13 and 83)

Figure 1. Chemical structures of telechelic PDMS samples investigated in this study. DP indicates the degree of polymerization.

long time and equilibrium concentration of open stickers is very low. Thus, the bond dissociation time becomes the major controlling parameter, network relaxation happens through the bond-hopping mechanism, and the bond rearrangement time becomes comparable to the bond dissociation time in this regime. However, this model's prediction for the high bond dissociation energy has not been thoroughly tested yet.

In this study, we tested the above model in the regime of high bond dissociation energy. We analyzed the dynamics of urea and S−COOH-functionalized telechelic poly(dimethyl siloxane) (PDMS) using dielectric spectroscopy, rheology, small-angle X-ray scattering (SAXS), and differential scanning calorimetry (DSC). While both functional groups bind each other through H-bonding, the interaction strength for urea is much higher than that of S−COOH. Broadband dielectric spectroscopy (BDS) was used to investigate the dynamics of these reversible interactions, and rheological measurements indicated the presence of a supramolecular chain in our investigated polymers. Analysis of the data revealed that the time scale of the bond dissociation and terminal relaxation are the same for the urea-functionalized telechelic systems, whereas for S−COOH-functionalized chains, they differ by up to 3 orders of magnitude. Detailed analysis of all the data revealed that the bond lifetime renormalization model indeed describes well the behavior of the studied systems in both intermediate and high dissociation energy regimes.

MATERIALS AND METHODS

The chemical structures of the investigated PDMS telechelic polymers are shown in Figure 1.

Synthesis of the Telechelic PDMS Polymers. *Urea-Functionalized PDMS.* 3.0 g (3 mmol) of aminopropyl-terminated PDMS (DMS-A11, Gelest) was added into a flame-dried 100 mL round-bottom flask with a magnetic stir bar inside. The flask was connected to a Schlenk line under vacuum at 50 °C for 30 min to remove water, and the flask was then transferred into a glovebox. 15 mL of anhydrous dichloromethane was added to dissolve PDMS under magnetic stirring. 0.47 g (6.6 mmol) of ethyl isocyanate dissolved in 5 mL of anhydrous dichloromethane was added into the flask dropwise under stirring. After 2 h of reaction, the mixture was removed from the glovebox. A rotary evaporator was used to remove the solvent and extra ethyl isocyanate. ^{1}H NMR results are shown in the Supporting Information (Figure S1).

Carboxylic Acid-Terminated PDMS. Synthesis of the carboxylic acid-terminated PDMS (PDMS-S-COOH) sample has been described earlier.[19] As an example, 3 g (0.5 mmol) of vinyl-terminated PDMS (Gelest) with a molecular weight (MW) of 6000 g/mol and 0.2123 g (2 mmol) of 3-mercaptopropionic acid were dissolved in 10 mL of anhydrous toluene. 0.041 g (0.25 mmol) of recrystallized 2,20-azobis(2-methylpropionitrile) (Sigma-Aldrich) was dissolved in 3 ml of toluene and added to the polymer mixture. The mixture was kept overnight at 65 °C under an argon atmosphere. After evaporation of the solvents, hexane was used to wash the product. Subsequently, hexane was evaporated, followed by dialysis against dichloromethane to remove low-molecular-weight impurities.

BDS Measurements. Before BDS measurement, all samples were dried in a vacuum oven at 333 K for 1 day to remove solvent and moisture. Then, BDS spectra in the frequency range from 10^{-2} to 10^{6} Hz were measured using a Novocontrol system that includes an Alpha-A impedance analyzer and a Quatro Cryosystem temperature control unit. DP 22 and DP 50 urea-functionalized PDMS (PDMS-U) were placed into a parallel-plate dielectric cell made of sapphire and invar steel with an electrode diameter of 10 mm and a capacitance of 3.3 pF with an electrode separation of 210 μm. The PDMS-S-COOH samples were measured in a capacitor composed of two gold-plated electrodes of 20 mm diameter separated by a Teflon spacer of 34.4 μm thickness. To prevent crystallization, all samples were quenched from room temperature to about 113 K and reheated to 10 K below the T_g before the measurements. All spectra were measured on heating. After each temperature increase, the samples were equilibrated for 10 min to reach thermal stabilization within 0.1 K.

Rheological Measurements. Small amplitude oscillatory shear (SAOS) measurements were conducted with the strain-controlled mode of an AR2000ex rheometer (TA Instruments) in the angular frequency range of 10^{2}−10^{-1} rad s^{-1} utilizing parallel plate geometry. Plate diameters of 4 and 8 mm were employed, depending on the magnitude of the shear modulus. The gap distance between the top and bottom plate was approximately 0.5 mm and kept constant throughout the temperature range. Prior to the measurement, each sample was dried as described for the BDS measurements. A strain sweep was conducted before each spectral sweep to determine the appropriate strain, keeping the SAOS in the linear regime. Before each scan, the samples were thermally equilibrated for 10 min; the maximum permitted temperature deviation was 0.2 K.

SAXS Measurements. X-ray scattering spectra for all studied samples as well as the reference sample PDMS-CH_3 were measured in the way described previously.[26] The samples were measured on XEUSS 3.0 (Xenocs, France) equipped with a Cu Kα microfocus source and a Pilatus 300 k detector (Dectris, Switzerland). The scattering vector (q) was calibrated by silver behenate standard material. The distances between the sample and the detector were 0.9 and 0.55 m for SAXS and WAXS, respectively. The sample was squeezed into a capillary tube made of quartz glass with a diameter of 1.5 mm and a wall thickness of 0.01 mm. The capillary was placed perpendicular to the X-ray beam.

https://doi.org/10.1021/acs.macromol.2c02446
Macromolecules 2023, 56, 2397−2405

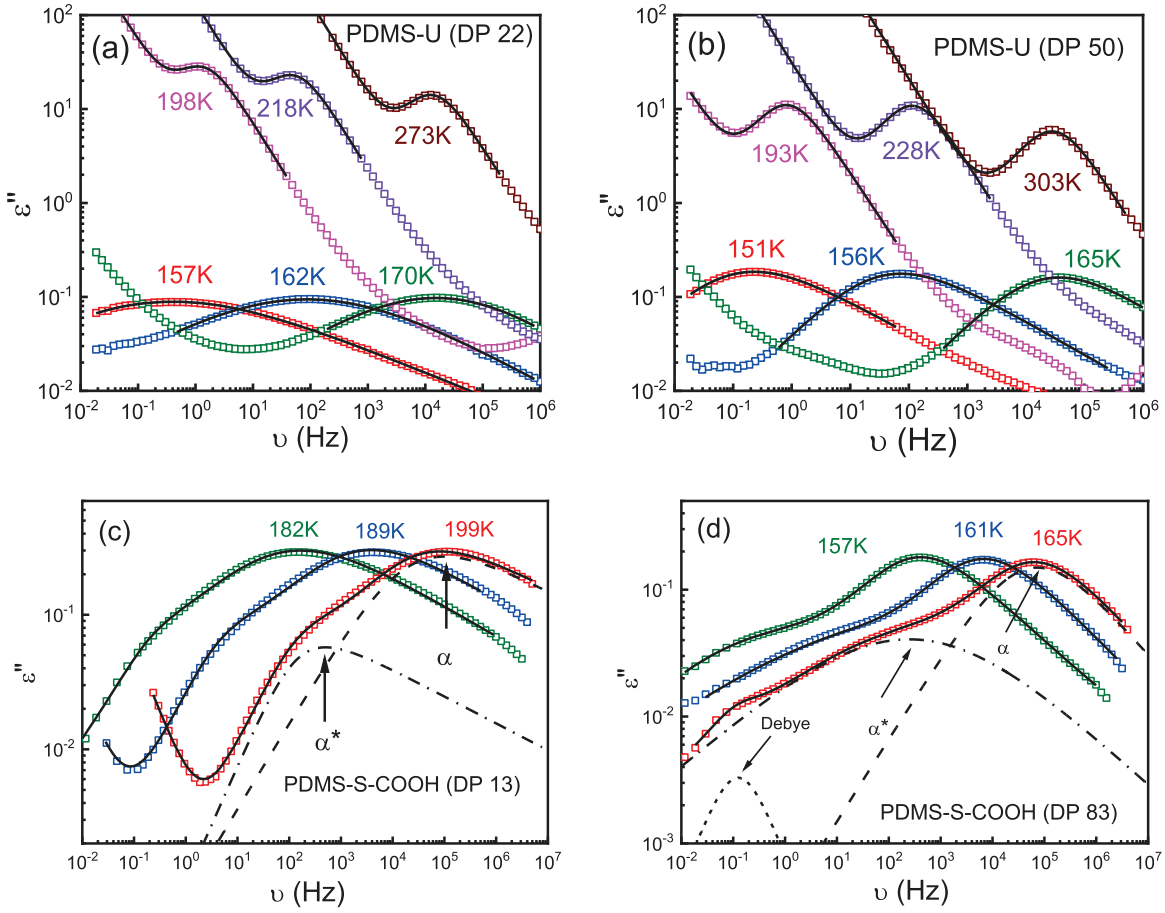

Figure 2. Dielectric loss spectra of (a) PDMS-U (DP 22), (b) PDMS-U (DP 50), (c) PDMS-S-COOH (DP 13), and (d) PDMS-S-COOH (DP 83). The solid lines present the total fit. The dashed lines present the fits of the α relaxation process. The dash-dotted line presents the fit of the α^*-relaxation process. The short dashed line in (d) presents the fit for the Debye-like process for the PDMS-S-COOH (DP 83) sample.

The measurement was also done on the empty capillary to subtract the background. X-ray measurements were performed at room temperature.

X-ray scattering spectra for PDMS-U (DP 22, DP 50), PDMS-S-COOH (DP 83, DP 13), and PDMS-CH_3 are shown in Figure S3 in the Supporting Information. For all samples, a strong and sharp peak is observed at $q \sim 0.85$ Å^{-1}; it reflects spatial correlations between PDMS segments, while the weaker peak around $q \sim 1.5$ Å^{-1} reflects intra-segmental correlations.[27] The introduction of functional groups did not change the X-ray spectra, and no additional scattering appears at low q, indicating no measurable micro-phase separation. Additionally, DSC curves of these samples also showed a single T_g value in the heat flow spectra (Figure S2), which is around the glass transition range of the PDMS segments, further confirming no micro-phase separation in the studied samples.

RESULTS

Two dielectric processes were observed for PDMS-U samples (Figure 2a,b). They are strongly separated in time and appear in the studied frequency range at different temperatures. To fit the loss spectra and to analyze the relaxation times of these processes, the phenomenological Havriliak–Negami (HN) function is used.[28]

$$\varepsilon''(\upsilon) = -\mathrm{Im}\sum_{k=1}^{n}\left\{\frac{\Delta\varepsilon_k}{[1+(2\pi i\upsilon\tau_{\mathrm{HN},k})^{\beta_k}]^{\gamma_k}}\right\} + \frac{\sigma}{2\pi\upsilon\varepsilon_0} \quad (1)$$

Here, ε_0 is the vacuum permittivity, $\Delta\varepsilon$ denotes the dielectric relaxation strength, β and γ represent the shape parameters, τ_{HN} is HN relaxation time, and k indicates the number of processes. The second term in eq 1 considers the conductivity (σ) contribution to the loss spectra at higher temperatures. This fit reveals two surprising results for the slow relaxation process. First, the shape of this process is of Debye type ($\beta \approx \gamma \approx 1$), which is unusual for polymers but is prevalent in monohydroxy alcohols[29−31] and some secondary amides.[32] Second, it has a relatively high dielectric strength, ~2 orders higher than the PDMS backbone. Indeed, urea has quite a high dipole moment, ~6.5−7.5 Debye.[33,34] For comparison, the dipole moment per repeating unit of PDMS is ~0.29 to 0.33 Debye.[35,36] In addition, multiple hydrogen bonds are involved in the bond exchange process, which might provide an additional enhancement of the dielectric strength, and the Debye process in mono-alcohols is known to have high strength.[29−31]

BDS spectra for the PDMS-S-COOH sample with DP 83 and DP 13 are shown in Figure 2c,d. While the BDS spectra of the sample with DP 13 can be well described using only two peaks, a third peak is required to describe the spectra of the DP 83 sample (Figure 2d). So, the spectra of the samples were fit to eq 1 with 2 HN functions for the DP 13 sample and 3 HN functions for the DP 83 sample. The analysis revealed that the slowest relaxation peak in the spectra of the DP 83 sample also has a Debye-like shape.

The peak position of the dielectric loss spectra was used to estimate the characteristic relaxation time of these processes.

https://doi.org/10.1021/acs.macromol.2c02446
Macromolecules 2023, 56, 2397−2405

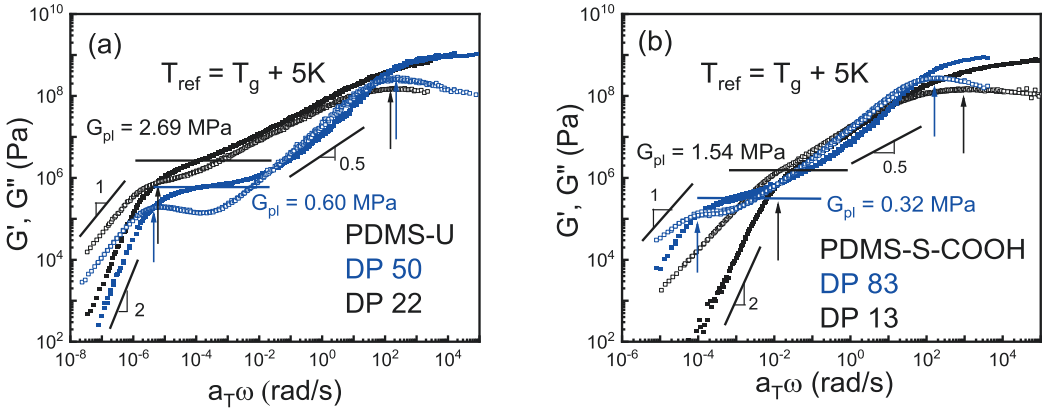

Figure 3. (a) Shear modulus master curves for (a) PDMS-U with DP 50 (blue) and DP 22 (black) and (b) PDMS-S-COOH with DP 83 (blue) and DP 13 (black) against the radial frequency at a reference temperature of T_g + 5 K. The solid symbols present G', while the open symbols present the G'' spectra. The rubbery plateau modulus levels, G_{pl}, are shown by the solid lines. The peak at higher frequency is related to the segmental relaxation of the PDMS backbones, whereas the peak at lowest frequency indicates the terminal relaxation of the samples.

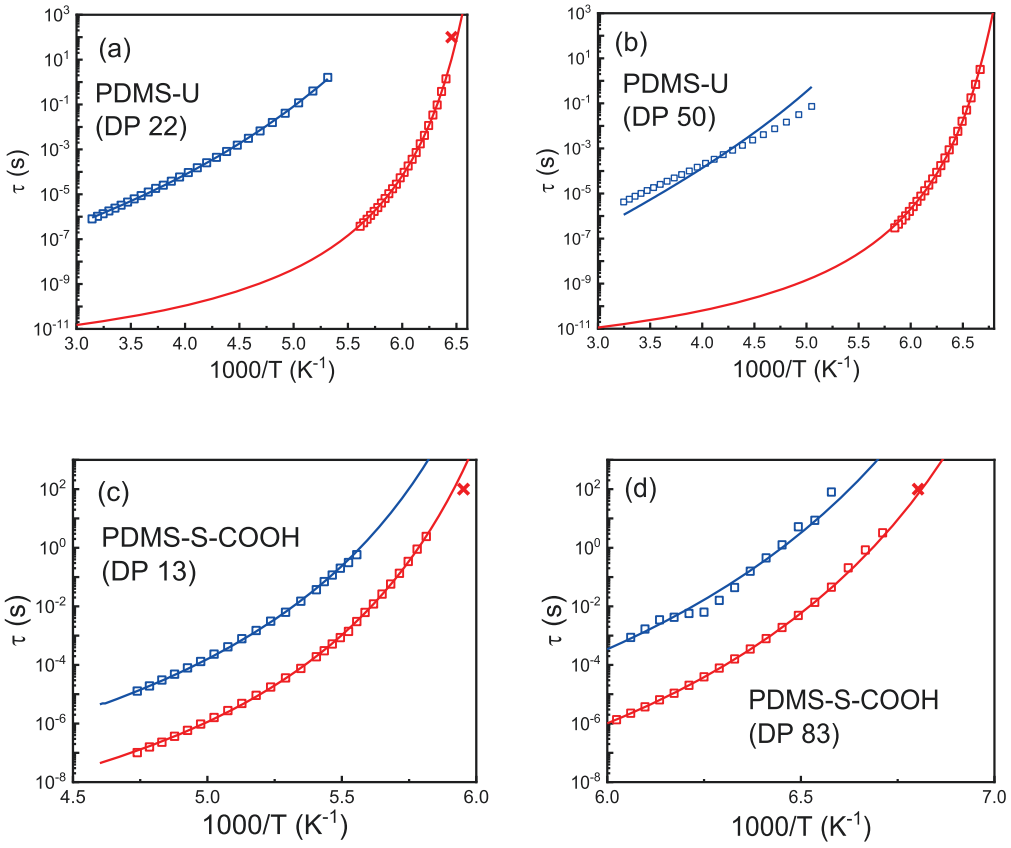

Figure 4. Temperature dependence of the relaxation time for segmental α-relaxation (red squares) and the α*-relaxation (blue squares) for the PDMS-U sample with (a) DP 22 and (b) DP 50 and for PDMS-S-COOH samples with (c) DP 13 and (d) DP 83. Red crosses mark T_g of the samples estimated from the heat flow curve from DSC (Figure S2). The red lines show VFT fits (eq 3), while the blue lines show the fits to eq 4.

The relaxation time corresponding to the peak position (τ_{max}) is directly related to τ_{HN}[37]

$$\tau_{max} = \tau_{HN}\left[\sin\left(\frac{\beta_k\pi}{2+2\gamma_k}\right)\right]^{-1/\beta}\left[\sin\left(\frac{\beta_k\gamma_k\pi}{2+2\gamma_k}\right)\right]^{1/\beta} \quad (2)$$

In the case of the Debye-like peak, the characteristic relaxation time $\tau_{max} = \tau_{HN}$.

Rheological data were used to create a master curve assuming time−temperature superposition by horizontal shifting of shear modulus spectra measured at several temperatures (Figure 3). Although time−temperature superposition usually does not work in these systems, the obtained master curves provide good qualitative representation of the frequency dependence of the shear modulus. The process at high frequencies corresponds to the segmental relaxation (storage modulus values between 0.1 and 1 GPa). At the lowest frequencies, an additional process appears with the distinctive slopes of 2 and 1 for $G'(\omega)$ and $G''(\omega)$ (in double-logarithmic representation), respectively. This is typical of the terminal relaxation process, which indicates

https://doi.org/10.1021/acs.macromol.2c02446
Macromolecules 2023, 56, 2397−2405

macroscopic stress relaxation in the system. Since the terminal relaxation in the master curve might be affected by the breakdown of TTS, the characteristic time for the terminal relaxation (τ_C) is estimated based on the crossover frequency of $G'(\omega)$ and $G''(\omega)$ only when it is in the frequency window of the rheometer. In addition, we observed a rubbery plateau in between these two processes, which is of the order of 1 MPa, especially for the PDMS-U (DP 50). We also notice that the shape of the curve is analogous to that of polydisperse polymer melt. This indicates the formation of long chains via transient hydrogen bonds between functional chain ends. In such cases, both the reptation dynamics and the kinetics of transient bond breaking and formation control the terminal relaxation time.[38]

DISCUSSION

We start the discussion with assignments of the relaxation processes observed in the dielectric spectra. Figure 4 presents the characteristic time of the dielectric processes in the samples studied here. The highest frequency peak in all samples can be assigned to the PDMS segmental relaxation (α-process) because its characteristic relaxation time extrapolated to $\tau \sim 100$ s agrees well with T_g estimated from DSC (Figure S2). Following earlier studies,[39] we name the slower relaxation process as α^*-process. It should be related to the bond dissociation process because H-bond dissociation changes the dipole moment. Indeed, the amplitude of this process increases with the increase of the end-group fraction (Figure 2). The assignment of the slowest process in the PDMS-S-COOH sample with DP 83 will be discussed later.

The temperature dependence of segmental relaxation time can be fit by the usual Vogel−Fulcher−Tammann (VFT) equation (Figure 4)[40,41]

$$\tau_\alpha(T)=\tau_0\exp\left(\frac{B}{T-T_0}\right) \tag{3}$$

where τ_0 is the high temperature limit of the segmental relaxation time, and B and T_0 are the VFT parameters. To minimize the number of the free fit parameters, we fixed $\tau_0 = 10^{-12}$ s. The fit parameters are presented in Table 1.

Table 1. VFT Fit Parameters (B and T_0) of the Segmental Relaxation, Activation Energy of Bond Dissociation (E_a) Estimated Using eq 5, and the Value of $2RT \ln N$ at $T = 200$ K for PDMS-U and PDMS-S-COOH Samples

sample	B	T_0	$2RT \ln N$ (kJ/mol)	E_a (kJ/mol)
PDMS-U DP 22	530	137	6.4	28 ± 1
PDMS-U DP 50	485	133	9.2	31 ± 1
PDMS-S-COOH DP 13	762	145	4.7	8 ± 0.5
PDMS-S-COOH DP 83	479	132	10.9	8 ± 0.5

To estimate the activation energy of bond dissociation E_a, many authors used the apparent activation energy estimated from the temperature dependence of the α^*-process. This is not correct because the dissociation of the bond in this case depends on the polymer segmental motions.[19,21,42] For a dynamic bond to dissociate, the connected segment needs to move, and the attempt time for the bond dissociation should be comparable to the segmental relaxation time. In other words, the bond dissociation process requires motion of functional groups that is controlled by the segmental friction coefficient. Thus, the temperature dependence of segmental relaxation time should be explicitly taken into account for calculations of E_a.[19,21,42]

$$\tau_{\alpha^*}(T) = \tau_\alpha(T)\exp\left(\frac{E_a}{RT}\right) \tag{4}$$

The fits of the $\tau_\alpha{}^*(T)$ to eq 4 are presented in Figure 4, and the values obtained from the fit energy barrier for bond dissociation, E_a, are presented in Table 1. One can rewrite eq 4 and estimate the dissociation energy from the ratio of $\tau_\alpha{}^*(T)/\tau_\alpha(T)$

$$E_a = RT\ln\left[\frac{\tau_{\alpha^*}(T)}{\tau_\alpha(T)}\right] \tag{5}$$

The overlap of the data for relaxation times of α^* and α processes in the case of urea-terminated samples is very limited (Figure 4). So, we used VFT fits of the τ_α data extrapolated toward a higher temperature for analysis of these data. This analysis revealed a surprisingly good description of the ratio of relaxation times by the Arrhenius approximation (Figure 5). Slight deviation from linear behavior observed for the sample with DP 50 (Figure 5b) can be the result of the VFT extrapolation. The observed behavior is in contrast to several other examples where strong deviation from the simple Arrhenius relationship was observed and discussed.[23,43]

A linear fit of $\ln\left[\frac{\tau_{\alpha^*}(T)}{\tau_\alpha(T)}\right]$ vs $1/T$ allows estimates of enthalpic ΔH and entropic ΔS contributions to the energy barrier of the bond dissociation in PDMS-U samples

$$\frac{E_a}{RT} = \frac{\Delta H}{RT} - \frac{\Delta S}{R} = \ln\left[\frac{\tau_{\alpha^*}(T)}{\tau_\alpha(T)}\right] \tag{6}$$

This fit (Figure 5) revealed dominating enthalpic contributions with $\Delta H \sim 26.5$ kJ/mol for DP 22 to ~23.1 kJ/mol for DP 50, while relatively small entropic contribution ($T\Delta S$ at the relevant $T = 250$ K) increases with the increase of the chain length from ~1.5 kJ/mol for DP 22 to ~7.7 kJ/mol for DP 50.

The estimated E_a for the urea-terminated samples (Figure 5, Table 1) is significantly higher than the energy barrier for PDMS-S-COOH samples obtained earlier,[19] $E_a \sim 8$ kJ/mol (Figure 4, Table 1). The latter value is reasonable for a single hydrogen bond. However, the value estimated for the urea dissociation suggests breaking 3−4 hydrogen bonds, which is possible to form for these structural units (Figure 1).

As the next step, we compare the bond rearrangement time estimated from rheology (terminal relaxation time) to the bond dissociation time estimated from the dielectric data (α^*-process). For direct comparison of these time scales, the dielectric data should be also analyzed in the modulus presentation.[44] So, the dielectric spectra were converted to the dielectric loss modulus $M''(\omega)$ according to[37]

$$M^*(\omega) = \frac{1}{\varepsilon^*(\omega)} = M'(\omega) + iM''(\omega) \tag{7}$$

and fit to the same HN function (eq 1). The so-obtained $\tau_\alpha{}^*{}_{-M}$ appears different from $\tau_\alpha{}^*$ estimated from the permittivity loss spectra for PDMS-U samples due to the high amplitude of the α^*-process[44] (Figures 2 and S4). There is no significant difference between these time scales in the case of PDMS-S-COOH samples due to the relatively weak strength of this process[44] (Figures 2 and S4).

https://doi.org/10.1021/acs.macromol.2c02446
Macromolecules 2023, 56, 2397−2405

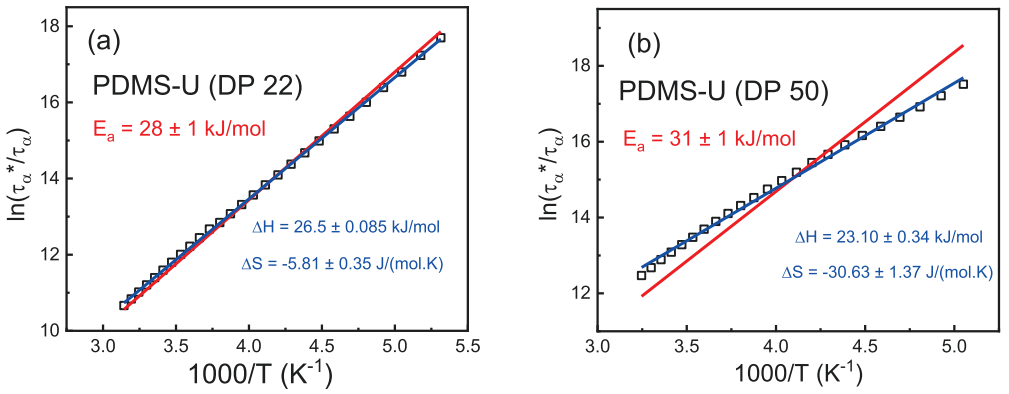

Figure 5. Ratio of the time scales $\tau_\alpha^*(T)$ and $\tau_\alpha(T)$ against 1000/T for PDMS-U with (a) DP 22 and (b) DP 50. The red lines present the Arrhenius law fit (eq 5), and the blue lines present the linear fit, accounting for the entropic contribution (eq 6). Comparison of the fits suggests that the entropic contribution is relatively small.

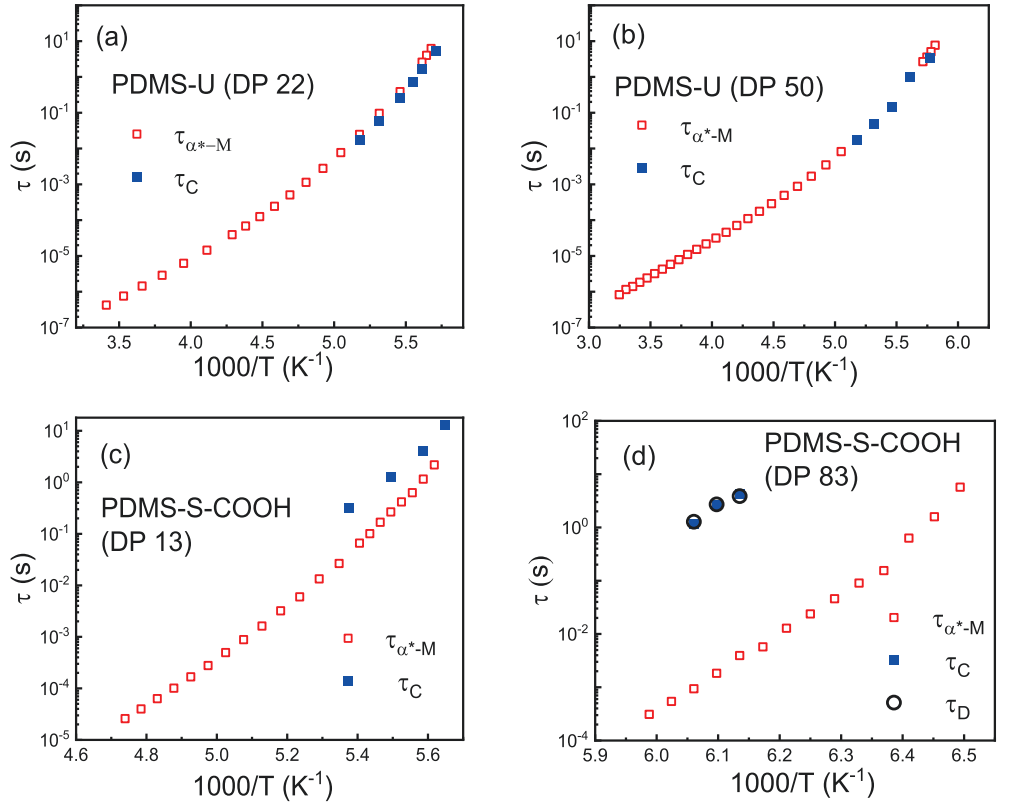

Figure 6. Comparison of dielectric modulus τ_{α^*-M} (red open squares) and rheological τ_C (blue closed squares) relaxation times for (a) PDMS-U DP 22, (b) PDMS-U DP 50, (c) PDMS-S-COOH DP 13, and (d) PDMS-S-COOH DP 83 samples. For the PDMS-S-COOH DP 83 sample, the Debye-like process time τ_D (black open circle) is also included.

Direct comparison (Figure 6) reveals very good agreement between the rheological and dielectric modulus timescales for both PDMS-U samples. This result suggests that the bond dissociation time process observed in the dielectric spectra of these samples is essentially the same as the bond rearrangement time. Rheological time appears only slightly slower than the dielectric modulus time in PDMS-S-COOH with DP 13 (Figure 6c), while it is almost 1000 times slower in the sample with DP 83 (Figure 6d). Surprisingly, the relaxation time of the slowest dielectric process observed in the DP 83 sample agrees well with the terminal relaxation time (Figure 6d). Thus, the slowest dielectric relaxation process in the PDMS-S-COOH sample with DP 83 reflects the bond rearrangement time, and it also has the Debye-like shape as is observed for the α^*-process in the PDMS-U samples.

Based on the obtained values of E_a, we can relate the bond strength regime of each sample to the criterion introduced by the bond-lifetime renormalization model[24] (Table 1). To estimate the number of segments N, we assume $N = 2 \times \mathrm{DP}/C_\infty \approx \mathrm{DP}/3.15$ (we used the characteristic value $C_\infty = 6.3$[45]). PDMS-S-COOH with DP 83 is the only sample with the bond strength well within the intermediate regime, $RT \ln N < E_a < 2\,RT \ln N$ (Table 1), and our earlier detailed studies indeed revealed that the difference between the bond dissociation time τ_{α^*-M} and the bond rearrangement time τ_C can be well explained by the bond lifetime renormalization model.[19] Although

https://doi.org/10.1021/acs.macromol.2c02446
Macromolecules 2023, 56, 2397−2405

dissociation energy is essentially the same for the PDMS-S-COOH sample with DP 13 (Table 1), the much shorter chain brings it to the border of the strong interaction regime ($E_a > 2RT$ ln N), and the observed close values of τ_{α^*-M} and τ_C in the dynamics of this sample (Figure 6c) are in good agreement with the predictions of the model. In contrast, dissociation energy is very high for urea-terminated chains, and both PDMS-U samples are deep in the strong dissociation energy regime (Table 1). The observed very good agreement of the terminal relaxation time and the dielectric modulus time for the bond dissociation process (Figure 6a,b) is also in perfect agreement with the predictions of the bond lifetime renormalization model. Thus, indeed in the strong dissociation energy regime, the bond dissociation time and bond rearrangement time appear very similar. This justifies the use of mechanical relaxation time for estimates of the bond dissociation energy in the strong interaction regime. However, segmental relaxation should be explicitly taken into account for a good quantitative analysis.

We want to comment specifically on eq 4. Although it seems like a reasonable approximation, there are many experimental data which question its simplicity, demonstrating that the ratio of bond dissociation (or rearrangement) time to the segmental relaxation time decreases upon cooling.[23,43,46] The latter contradicts eq 4 and requires deeper understanding of the relationship between friction imposed on the stickers by the surrounding polymer matrix and the bond dissociation process. Recently, Schweizer and co-workers suggested that friction might follow weaker dependence on $\tau_\alpha(T)$ than the one predicted by eq 4,[43] and this puzzle remains unsolved. However, in the case of systems studied here, the bond dissociation temperature dependence seems to follow eq 4 reasonably well (Figure 4) and provides reasonable estimates of the energy barrier for bond dissociation.

Rheological measurements of the investigated polymers also show a rubbery plateau in their shear modulus master curves (Figure 3), although molecular weight of our chains is significantly below the entanglement molecular weight of PDMS (M_e ~10−12 kg/mol[47]). This indicates the formation of supramolecular polymer chains. From the viscosity measurements (Figure 7), it was observed that the viscosity of PDMS-U samples is ~1000 times higher than its non-associating counterpart, while it is only ~10 times higher in the case of PDMS-S-COOH samples. This is reasonable because the interaction strength is much higher in urea-functionalized samples than in the PDMS-S-COOH samples, and this leads to the formation of significantly longer transient chains.

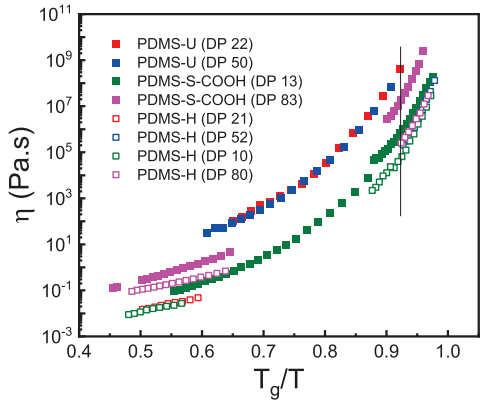

Figure 7. Comparison of the shear viscosity of PDMS-U and PDMS-S-COOH samples to the viscosity of their non-associated counterpart PDMS-H with comparable DPs. The temperatures are scaled with T_g of the samples. Crystallization of samples leads to the gap in some data.

One intriguing feature of the systems investigated in this study is the shape of the bond dissociation process in the dielectric spectra. It appears to have a Debye-like shape (single exponential relaxation) which is very unusual for polymers but is well documented for monohydroxy alcohols (MA) and secondary amides. The molecular origin of the Debye peak in these systems remains controversial. The Debye-like dielectric process has been also observed in short hydroxyl-terminated PDMS chains.[48] In our previous studies[39,49] and also in the case of PDMS-S-COOH samples presented here, the dielectric process of bond dissociation appears strongly stretched (Figure 2). However, in all these cases the bond rearrangement time was much longer than the bond dissociation time. In the examples studied here, the Debye process appears in the dielectric spectra at the timescale of terminal relaxation, i.e., bond rearrangement time. It is especially illustrative in the example of PDMS-S-COOH with DP 83, where the Debye-like dielectric relaxation process appears exactly at the terminal relaxation time which is much longer than the bond dissociation time (Figure 6d). However, currently we do not have any clear explanation for why the bond rearrangement process in the dielectric spectra appears with a Debye-like shape.

CONCLUSIONS

In this study, we investigated dielectric and rheological properties of telechelic PDMS polymers having two different functional groups forming hydrogen bonds. The activation energy of the bond dissociation process in these systems has been estimated using dielectric spectroscopy. The choice of functional groups and chain length enables the experimental test of the bond lifetime renormalization model in the strong and intermediate association regimes. Our analysis revealed good agreement of the experimental data with the model predictions. Most of the current studies use the rheological terminal relaxation time scales to estimate the energy barrier for bond dissociation. In general, this is not correct because rheology actually measures bond rearrangement time, not bond dissociation. The difference between the bond dissociation and bond rearrangement times can be well explained by the bond lifetime renormalization model. Our results clearly show that the use of terminal relaxation to estimate the bond dissociation energy is only valid in the strong interaction regime where both bond dissociation and bond rearrangement times become comparable. Our results also show very clearly that segmental relaxation should be taken explicitly into account for the estimation of bond dissociation energy, at least, in the case of the systems studied here.

Rheological measurements indicate that the viscoelastic properties of the associated polymers deviate considerably from their non-associating counterpart due to the formation of supramolecular chains with no phase separation. High dissociation energy of urea groups leads to the formation of superchains with effective length far exceeding the length of the telechelic chains. It remains a challenge to understand why the bond rearrangement process appears in the dielectric spectra with a Debye-like shape.

https://doi.org/10.1021/acs.macromol.2c02446
Macromolecules 2023, 56, 2397−2405

■ ASSOCIATED CONTENT

Supporting Information

The Supporting Information is available free of charge at https://pubs.acs.org/doi/10.1021/acs.macromol.2c02446.

NMR and DSC results for PDMS-U samples, SAXS data, and comparison of dielectric modulus and permittivity spectra (PDF)

■ AUTHOR INFORMATION

Corresponding Author

Alexei P. Sokolov − *Department of Chemistry, University of Tennessee, Knoxville, Tennessee 37996, United States; Chemical Sciences Division, Oak Ridge National Laboratory, Oak Ridge, Tennessee 37830, United States;* orcid.org/0000-0002-8187-9445; Email: sokolov@utk.edu

Authors

Sirui Ge − *Department of Material Science and Engineering, University of Tennessee, Knoxville, Tennessee 37996, United States;* orcid.org/0000-0002-4276-7838

Gregory Peyton Carden − *Department of Chemistry, University of Tennessee, Knoxville, Tennessee 37996, United States;* orcid.org/0000-0001-6229-6538

Subarna Samanta − *Department of Chemistry, University of Tennessee, Knoxville, Tennessee 37996, United States*

Bingrui Li − *The Bredesen Center for Interdisciplinary Research and Graduate Education, University of Tennessee, Knoxville, Tennessee 37996, United States;* orcid.org/0000-0002-4974-5826

Ivan Popov − *Department of Chemistry, University of Tennessee, Knoxville, Tennessee 37996, United States;* orcid.org/0000-0002-7235-2043

Peng-Fei Cao − *State Key Laboratory of Organic-Inorganic Composites, Beijing University of Chemical Technology, Beijing 100029, China;* orcid.org/0000-0003-2391-1838

Complete contact information is available at: https://pubs.acs.org/10.1021/acs.macromol.2c02446

Notes

The authors declare no competing financial interest.

■ ACKNOWLEDGMENTS

We thank the NSF Polymer Program for providing financial support to this study (BDS, rheology, DSC, and data analysis) under award DMR-1904657. B.L. and P.-F.C. acknowledge the support offered by the DOE BES Materials Science and Technology Division for synthesis. X-ray measurements were enabled by the Major Research Instrumentation Program of the National Science Foundation under award no. DMR-1827474.

■ REFERENCES

(1) Brunsveld, L.; Folmer, B. J.; Meijer, E. W.; Sijbesma, R. P. Supramolecular polymers. *Chem. Rev.* **2001**, *101*, 4071−4098.

(2) Amabilino, D. B.; Smith, D. K.; Steed, J. W. Supramolecular materials. *Chem. Soc. Rev.* **2017**, *46*, 2404−2420.

(3) Lehn, J. M. Supramolecular chemistry - Molecular information and the design of supramolecular materials. *Makromolekulare Chemie. Macromolecular Symposia*; Wiley Online Library, 1993; Vol. *69*, pp 1−17.10.1002/masy.19930690103

(4) Binder, W. H.; Zirbs, R. Supramolecular polymers and networkswith hydrogen bonds in the main-and side-chain. *Hydrogen bonded polymers* **2006**, *207*, 1−78.

(5) Wu, S.; Cao, X.; Zhang, Z.; Chen, Q.; Matsumiya, Y.; Watanabe, H. Molecular design of highly stretchable ionomers. *Macromolecules* **2018**, *51*, 4735−4746.

(6) Yount, W. C.; Loveless, D. M.; Craig, S. L. Small-molecule dynamics and mechanisms underlying the macroscopic mechanical properties of coordinatively cross-linked polymer networks. *J. Am. Chem. Soc.* **2005**, *127*, 14488−14496.

(7) Burattini, S.; Colquhoun, H. M.; Fox, J. D.; Friedmann, D.; Greenland, B. W.; Harris, P. J.; Hayes, W.; Mackay, M. E.; Rowan, S. J. A self-repairing, supramolecular polymer system: healability as a consequence of donor−acceptor $\pi-\pi$ stacking interactions. *Chem. Commun.* **2009**, 6717−6719.

(8) Cordier, P.; Tournilhac, F.; Soulié-Ziakovic, C.; Leibler, L. Self-healing and thermoreversible rubber from supramolecular assembly. *Nature* **2008**, *451*, 977−980.

(9) Li, B.; Zhao, S.; Zhu, J.; Ge, S.; Xing, K.; Sokolov, A. P.; Saito, T.; Cao, P.-F. Rational polymer design of stretchable poly (ionic liquid) membranes for dual applications. *Macromolecules* **2020**, *54*, 896−905.

(10) Lessard, J. J.; Garcia, L. F.; Easterling, C. P.; Sims, M. B.; Bentz, K. C.; Arencibia, S.; Savin, D. A.; Sumerlin, B. S. Catalyst-free vitrimers from vinyl polymers. *Macromolecules* **2019**, *52*, 2105−2111.

(11) Cao, P. F.; Li, B.; Hong, T.; Townsend, J.; Qiang, Z.; Xing, K.; Vogiatzis, K. D.; Wang, Y.; Mays, J. W.; Sokolov, A. P.; Saito, T. Superstretchable, Self-Healing Polymeric Elastomers with Tunable Properties. *Adv. Funct. Mater.* **2018**, *28*, 1800741.

(12) Rahman, M. A.; Bowland, C.; Ge, S.; Acharya, S. R.; Kim, S.; Cooper, V. R.; Chen, X. C.; Irle, S.; Sokolov, A. P.; Savara, A.; Saito, T. Design of tough adhesive from commodity thermoplastics through dynamic crosslinking. *Sci. Adv.* **2021**, *7*, No. eabk2451.

(13) Zhang, Z.; Ghezawi, N.; Li, B.; Ge, S.; Zhao, S.; Saito, T.; Hun, D.; Cao, P. F. Autonomous Self-Healing Elastomers with Unprecedented Adhesion Force. *Adv. Funct. Mater.* **2020**, *31*, 2006298.

(14) Pan, Y.; Ge, S.; Rashid, Z.; Gao, S.; Erwin, A.; Tsukruk, V.; Vogiatzis, K. D.; Sokolov, A. P.; Yang, H.; Cao, P.-F. Adhesive polymers as efficient binders for high-capacity silicon electrodes. *ACS Appl. Energy Mater.* **2020**, *3*, 3387−3396.

(15) Zhang, Z.; Luo, J.; Zhao, S.; Ge, S.; Carrillo, J.-M. Y.; Keum, J. K.; Do, C.; Cheng, S.; Wang, Y.; Sokolov, A. P.; Cao, P.-F. Surpassing the stiffness-extensibility trade-off of elastomers via mastering the hydrogen-bonding clusters. *Matter* **2022**, *5*, 237−252.

(16) Samanta, S.; Kim, S.; Saito, T.; Sokolov, A. P. Polymers with Dynamic Bonds: Adaptive Functional Materials for a Sustainable Future. *J. Phys. Chem. B* **2021**, *125*, 9389−9401.

(17) Grabowski, S. J. *Understanding Hydrogen Bonds: Theoretical and Experimental Views*; Royal Society of Chemistry, 2020.

(18) Li, Z.-T.; Wu, L.-Z. *Hydrogen Bonded Supramolecular Materials*; Springer, 2015.

(19) Ge, S.; Tress, M.; Xing, K.; Cao, P.-F.; Saito, T.; Sokolov, A. P. Viscoelasticity in associating oligomers and polymers: experimental test of the bond lifetime renormalization model. *Soft Matter* **2020**, *16*, 390−401.

(20) Van Ruymbeke, E. Preface: Special issue on associating polymers. *J. Rheol.* **2017**, *61*, 1099−1102.

(21) Zhang, Z.; Huang, C.; Weiss, R. A.; Chen, Q. Association energy in strongly associative polymers. *J. Rheol.* **2017**, *61*, 1199−1207.

(22) Gold, B. J.; Hövelmann, C. H.; Lühmann, N.; Székely, N. K.; Pyckhout-Hintzen, W.; Wischnewski, A.; Richter, D. Importance of Compact Random Walks for the Rheology of Transient Networks. *ACS Macro Lett.* **2017**, *6*, 73−77.

(23) Shabbir, A.; Javakhishvili, I.; Cerveny, S.; Hvilsted, S.; Skov, A. L.; Hassager, O.; Alvarez, N. J. Linear viscoelastic and dielectric relaxation response of unentangled UPy-based supramolecular networks. *Macromolecules* **2016**, *49*, 3899−3910.

(24) Stukalin, E. B.; Cai, L. H.; Kumar, N. A.; Leibler, L.; Rubinstein, M. Self-Healing of Unentangled Polymer Networks with Reversible Bonds. *Macromolecules* **2013**, *46*, 7525.

(25) Brassinne, J.; Cadix, A.; Wilson, J.; van Ruymbeke, E. Dissociating sticker dynamics from chain relaxation in supramolecular

polymer networks—The importance of free partner. *J. Rheol.* **2017**, *61*, 1123−1134.
(26) Ge, S.; Samanta, S.; Tress, M.; Li, B.; Xing, K.; Dieudonné-George, P.; Genix, A.-C.; Cao, P.-F.; Dadmun, M.; Sokolov, A. P. Critical Role of the Interfacial Layer in Associating Polymers with Microphase Separation. *Macromolecules* **2021**, *54*, 4246−4256.
(27) Mitchell, G. R.; Odajima, A. The local conformation of poly (dimethylsiloxane). *Polym. J.* **1984**, *16*, 351−357.
(28) Havriliak, S.; Negami, S. A complex plane representation of dielectric and mechanical relaxation processes in some polymers. *Polymer* **1967**, *8*, 161−210.
(29) Gainaru, C.; Figuli, R.; Hecksher, T.; Jakobsen, B.; Dyre, J.; Wilhelm, M.; Böhmer, R. Shear-modulus investigations of monohydroxy alcohols: Evidence for a short-chain-polymer rheological response. *Phys. Rev. Lett.* **2014**, *112*, 098301.
(30) Bierwirth, S. P.; Honorio, G.; Gainaru, C.; Böhmer, R. Linear and nonlinear shear studies reveal supramolecular responses in supercooled monohydroxy alcohols with faint dielectric signatures. *J. Chem. Phys.* **2019**, *150*, 104501.
(31) Kremer, F.; Loidl, A. *The Scaling of Relaxation Processes*; Springer International Publishing, 2018.
(32) Gilchrist, J. Dielectric relaxation of Amines by inversion and internal rotation. *Chem. Phys.* **1982**, *65*, 1−17.
(33) Mukherjee, K.; Das, S.; Tarif, E.; Barman, A.; Biswas, R. Dielectric relaxation in acetamide+ urea deep eutectics and neat molten urea: Origin of time scales via temperature dependent measurements and computer simulations. *J. Chem. Phys.* **2018**, *149*, 124501.
(34) Shi, M. W.; Thomas, S. P.; Hathwar, V. R.; Edwards, A. J.; Piltz, R. O.; Jayatilaka, D.; Koutsantonis, G. A.; Overgaard, J.; Nishibori, E.; Iversen, B. B.; Spackman, M. A. Measurement of Electric Fields Experienced by Urea Guest Molecules in the 18-Crown-6/Urea (1: 5) Host−Guest Complex: An Experimental Reference Point for Electric-Field-Assisted Catalysis. *J. Am. Chem. Soc.* **2019**, *141*, 3965−3976.
(35) Yamada, T.; Yoshizaki, T.; Yamakawa, H. Mean-square electric dipole moment of oligo-and poly (dimethylsiloxanes) in dilute solutions. *Macromolecules* **1992**, *25*, 1487−1492.
(36) Yamakawa, H.; Shimada, J.; Nagasaka, K. Statistical mechanics of helical wormlike chains. X. Dipole moments, electric birefringence, and electric dichroism. *J. Chem. Phys.* **1979**, *71*, 3573−3585.
(37) Kremer, F.; Schönhals, A. *Broadband Dielectric Spectroscopy*; Springer-Verlag: Berlin, 2003.
(38) Cates, M. Reptation of living polymers: dynamics of entangled polymers in the presence of reversible chain-scission reactions. *Macromolecules* **1987**, *20*, 2289−2296.
(39) Xing, K.; Tress, M.; Cao, P.; Cheng, S.; Saito, T.; Novikov, V. N.; Sokolov, A. P. Hydrogen-bond strength changes network dynamics in associating telechelic PDMS. *Soft Matter* **2018**, *14*, 1235−1246.
(40) Vogel, H. Das temperaturabhängigkeitsgesetz derviskosität von flüssigkeiten. *Phys. Z.* **1921**, *22*, 645−646.
(41) Tammann, G.; Hesse, W. Die Abhängigkeit der Viscosität von der Temperatur bie unterkühlten Flüssigkeiten. *Z. Anorg. Allg. Chem.* **1926**, *156*, 245−257.
(42) Chen, Q.; Tudryn, G. J.; Colby, R. H. Ionomer dynamics and the sticky Rouse model. *J. Rheol.* **2013**, *57*, 1441−1462.
(43) Ghosh, A.; Schweizer, K. S. Physical bond breaking in associating copolymer liquids. *ACS Macro Lett.* **2020**, *10*, 122−128.
(44) Richert, R.; Wagner, H. The dielectric modulus: relaxation versus retardation. *Solid State Ionics* **1998**, *105*, 167−173.
(45) Ding, Y.; Sokolov, A. P. Comment on the dynamic bead size and Kuhn segment length in polymers: Example of polystyrene. *J. Polym. Sci., Part B: Polym. Phys.* **2004**, *42*, 3505−3511.
(46) Tress, M.; Xing, K.; Ge, S.; Cao, P.; Saito, T.; Sokolov, A. What dielectric spectroscopy can tell us about supramolecular networks. *Eur. Phys. J. E: Soft Matter Biol. Phys.* **2019**, *42*, 133.
(47) Fetters, L.; Lohse, D.; Richter, D.; Witten, T.; Zirkel, A. Connection between polymer molecular weight, density, chain dimensions, and melt viscoelastic properties. *Macromolecules* **1994**, *27*, 4639−4647.
(48) Xing, K.; Chatterjee, S.; Saito, T.; Gainaru, C.; Sokolov, A. P. Impact of Hydrogen Bonding on Dynamics of Hydroxyl-Terminated Polydimethylsiloxane. *Macromolecules* **2016**, *49*, 3138−3147.
(49) Xing, K.; Tress, M.; Cao, P.-F.; Fan, F.; Cheng, S.; Saito, T.; Sokolov, A. P. J. M. The Role of Chain-End Association Lifetime in Segmental and Chain Dynamics of Telechelic Polymers. *Macromolecules* **2018**, *51*, 8561−8573.

https://doi.org/10.1021/acs.macromol.2c02446
Macromolecules 2023, 56, 2397−2405